



## Effect of solvent's types on the structure and magnetic properties of the as-coprecipitated $\text{Fe}_3\text{O}_4$ nanoparticles

Mahdi Madandar Motlagh, Seyyed Morteza Masoudpanah\*, Masoud Hasheminasari, Rasoul Beigdelou

School of Metallurgy & Materials Engineering, Iran University of Science and Technology (IUST), Tehran, Iran.

Received: 1 June 2018; Accepted: 07 October 2018

\* Corresponding author email: [masoodpanah@iust.ac.ir](mailto:masoodpanah@iust.ac.ir)

### ABSTRACT

Magnetite ( $\text{Fe}_3\text{O}_4$ ) nanoparticles were synthesized by coprecipitation route. Coprecipitation is a simple, reproducible and accessible technique relying on the coprecipitation of  $\text{Fe}^{2+}$  and  $\text{Fe}^{3+}$  cations by NaOH as base at low temperature ( $\sim 80^\circ\text{C}$ ). In this work, the role of different solvents ( $\text{H}_2\text{O}$ , ethylene glycol, diethylene glycol, triethylene glycol) on phase, structure, microstructure and magnetic properties were characterized by X-ray diffractometry, electron microscopy and vibrating sample magnetometry techniques. Single phase  $\text{Fe}_3\text{O}_4$  nanoparticles were crystallized in water and organic solvents. The particle size decreased from 53 to 33 nm by precipitating in the presence of organic solvents in contrast to water due to the introduction of more nucleation of particles caused by decrease in surface energy. Furthermore, the organic solvents prevent particle growth by adsorbing on the nucleus surface, leading to smaller particles. The as-coprecipitated  $\text{Fe}_3\text{O}_4$  nanoparticles exhibited ferromagnetic behavior without any coercivity, confirming the superparamagnetism. The maximum saturation magnetization ( $M_s$ ) of 54 emu/g was achieved for the as-coprecipitated  $\text{Fe}_3\text{O}_4$  nanoparticles using ethylene glycol as solvent, possibly due to their higher crystallinity. However, the  $M_s$  decreased to 41 and 45 emu/g for precipitation in the presence of diethylene glycol and triethylene glycol, respectively, due to the more particle size reduction, leading to the spin canting on the particle surface.

**Keywords:** Coprecipitation;  $\text{Fe}_3\text{O}_4$ ; Solvent; Magnetic properties.

### 1. Introduction

Superparamagnetic  $\text{Fe}_3\text{O}_4$  (and  $\gamma\text{-Fe}_2\text{O}_3$ ) nanoparticles have been used in many in-vitro and in-vivo biomedical applications like cells detection and separation, contrast agents in magnetic resonance imaging, magnetic targeted drug delivery and magnetic hyperthermia due to their considerable biocompatibility and magnetic properties [1, 2]. Magnetic hyperthermia relies on the heating of tumors by increasing their

local temperature (up to  $41\text{--}45^\circ\text{C}$ ) leading either to cell degradation or even to apoptotic death [3]. For magnetic hyperthermia, ferrimagnetic  $\text{Fe}_3\text{O}_4$  and  $\gamma\text{-Fe}_2\text{O}_3$  nanoparticles are mostly used as mediator for the local heat release under AC magnetic field, due to physiological stability, bearable biocompatibility and biodegradability [4]. Furthermore,  $\text{Fe}_3\text{O}_4$  and  $\gamma\text{-Fe}_2\text{O}_3$  nanoparticles should exhibit high saturation magnetization with a small particle size ( $\sim 20\text{--}40$  nm) and narrow

distribution to achieve high heating efficiency [5].

To date, superparamagnetic  $\text{Fe}_3\text{O}_4$  nanoparticles have been synthesized by co-precipitation, thermal decomposition, solvothermal syntheses, and biological synthesis methods [6, 7]. Among these methods, coprecipitation of  $\text{Fe}^{2+}$  and  $\text{Fe}^{3+}$  cations by a base such as NaOH and  $\text{NH}_4\text{OH}$  (below 80 °C) is a simple, reproducible and accessible technique for mass production of magnetite nanoparticles [8]. However, the use of expensive, toxic or incompatible aqueous precursors and solvents, the application of high temperature or pressure and costly equipments are major drawbacks for the other many wet chemical methodologies in terms of green and large-scale production. Wide particle size distribution caused by the uncontrolled aggregation of particles is a main disadvantage of coprecipitation method, leading to the lower heating efficiency [9]. Although the control of main parameters of the coprecipitation process such as type of salts (chlorides, sulfates and nitrates), pH and ionic strength enables reproducible synthesis of magnetite nanoparticles; the need for tuning particle size and its distribution necessitates the exploration of other approaches such as employment of the chelating and stabilizer agents (e. g. citric acid, oleic acid, dextran, polyvinyl alcohol (PVA), etc.), Ostwald ripening and electrostatic size sorting [10, 11]. For example, magnetite nanoparticles with sizes of 4–10 nm were stabilized in an aqueous solution of 1 wt% PVA [12].

In the coprecipitation method, water is used almost exclusively as solvent because of its exceptional ability to dissolve mineral salts [11]. The high polarity and high dielectric constant of water lead to the high solubility of ionic and covalent solids in water. However, water molecules can bridge the neighboring hydroxyl groups, resulting in hard agglomerations. Therefore, there are many efforts to use suitable organic/mixed solvents instead of water in spite of their higher cost [13]. Furthermore, the organic solvents can be adsorbed on the surface of coprecipitated nanoparticles ensuring the collide stability of the magnetite suspension and increased the air oxidation resistant of the magnetite nanoparticles [14-16].

In this study, we compared the solvents effect (water, ethylene glycol, diethylene glycol and triethylene glycol) on the structure, microstructure and magnetic properties of the coprecipitated magnetite nanoparticles.

## 2. Experimental procedures

Analytical grade of  $\text{FeCl}_2 \cdot 4\text{H}_2\text{O}$ ,  $\text{FeCl}_3 \cdot 6\text{H}_2\text{O}$ , NaOH, ethyleneglycol ( $\text{HOCH}_2\text{CH}_2\text{OH}$ ), diethylene glycol ( $\text{HOCH}_2\text{CH}_2\text{OCH}_2\text{CH}_2\text{OH}$ ) and triethylene glycol ( $\text{HOCH}_2\text{CH}_2\text{OCH}_2\text{CH}_2\text{OCH}_2\text{CH}_2\text{OH}$ ) were used as provided from Merck Co.

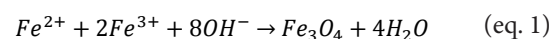
Magnetite nanoparticles were synthesized by chemical coprecipitation method. In this procedure, a mixed aqueous solution was prepared by dissolving required amounts of  $\text{FeCl}_2 \cdot 4\text{H}_2\text{O}$ ,  $\text{FeCl}_3 \cdot 6\text{H}_2\text{O}$  with the molar ratio of  $\text{Fe}^{3+}$  to  $\text{Fe}^{2+}$  as 2:1, in 20 mL distilled water, ethylene glycol, diethylene glycol and triethylene glycol. 20 mL aqueous solution of 8 M NaOH was used as the precipitating agent. Drops of metal chlorides and NaOH solutions were added from two separate burets into a reaction vessel containing 20 mL of distilled water. The resultant precipitation was collected and centrifuged at 5000 rpm and then washed with distilled water for several times.

Phase evolution was analyzed by PANalytical X'pert X-ray diffractometer (XRD) using monochromatic  $\text{CuK}\alpha$  radiation. Average crystallite size of the samples was also calculated from the width of (400) peak using Scherrer's equation. The (400) peak has suitably high intensity with no overlapping by other reflection peaks.

Morphology and microstructure of the  $\text{Fe}_3\text{O}_4$  nanoparticles were observed by TESCAN Vega II field emission scanning electron microscopy (FESEM). A vibrating sample magnetometer (VSM) (Meghnatis Daghigh Kavir Co., Iran) was also employed to measure the magnetic properties at room temperature with maximum field of 10 kOe.

## 3. Results and discussion

XRD patterns of the as-coprecipitated  $\text{Fe}_3\text{O}_4$  nanoparticles in water and various organic solvents are shown in Fig. 1. The (220), (311), (400), (422), (511) and (440) peaks related to the spinel structure with space group of  $\text{Fd}3\text{m}$  show the formation of black-colored single phase  $\text{Fe}_3\text{O}_4$  powders without any impurities. The  $\text{Fe}_3\text{O}_4$  was precipitated in the pH range of 9 to 14 as follows:



The iron hydroxides are initially precipitated during addition of NaOH as base. The hydroxides are condensed to form water, leading to the nucleation

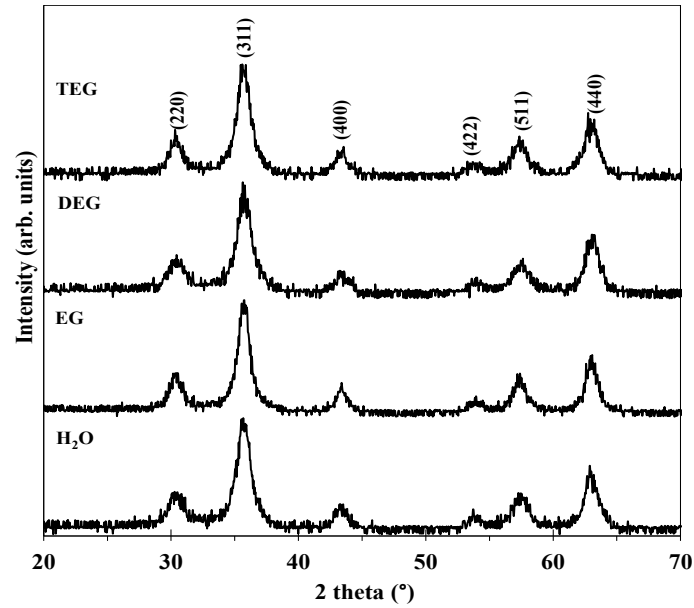


Fig. 1- XRD patterns of the as-coprecipitated powders in the various solvents.

Table 1- The crystallite size, magnetic size, lattice parameters and saturation magnetization of the as-coprecipitated Fe<sub>3</sub>O<sub>4</sub> powders

Solvents	Crystallite size (nm)	D <sub>M</sub> (nm)	a (Å)	Ms (emu/g)
H <sub>2</sub> O	16	13	8.3915	49
EG	14	13	8.3954	54
DEG	8	5	8.3900	45
TEG	7	5	8.3902	41
Fe <sub>3</sub> O <sub>4</sub> (JCPDS file No. 19-0629)			8.396	
γ-Fe <sub>2</sub> O <sub>3</sub> (JCPDS file No. 19-0629)			8.352	

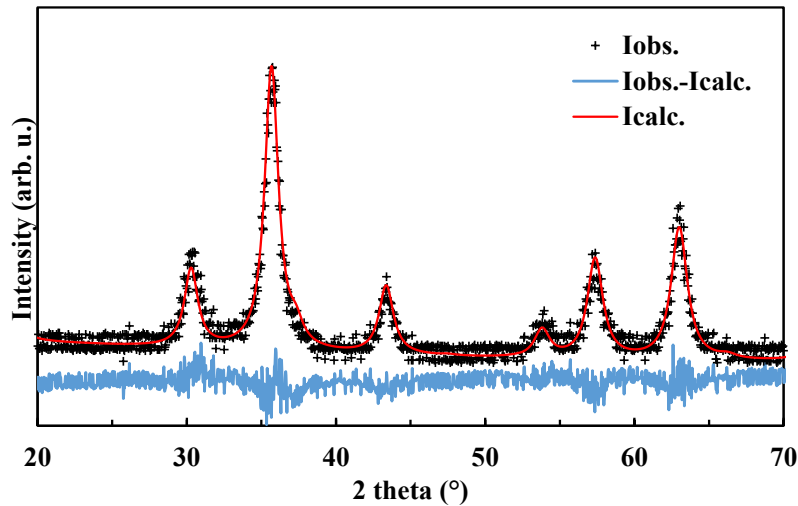


Fig. 2- XRD pattern and Rietveld refinement results of the as-coprecipitated powders in EG solvent. The fitting qualities, R<sub>exp</sub>, R<sub>wp</sub>, and χ<sup>2</sup> are 18%, 24%, and 1.34, respectively (Iobs. observed intensity, Icalc. calculated intensity, Iobs.-Icalc. the residual).

and growth of oxide phase [10]. The direct synthesis of magnetite without further treatment is due to the fast nucleation and growth processes. Table 1 shows the crystallite size, magnetic size and lattice parameter of the as-coprecipitated  $\text{Fe}_3\text{O}_4$  nanoparticles. The crystallite size decreased from 16 to 7 nm while using organic solvents, as can be confirmed by peak broadening of XRD reflections. The decrease in crystallite size can be attributed to the promotion of nucleation caused by the decrease of barrier energy [10]. The organic solvents with the hydroxyl groups increases the acidity of the reaction solution and then lowered solution-oxide interfacial energy and barrier energy for nucleation [17]. Furthermore, the organic molecules can be adsorbed on the nucleus, preventing them from growth [18].

XRD pattern and Rietveld refinement results

of the as-coprecipitated  $\text{Fe}_3\text{O}_4$  nanoparticles in ethylene glycol solvent are presented in Fig. 2. It is worth to note that the magnetite and maghemite have similar spinel structure and therefore cannot be easily distinguished. However, the lattice parameters (Table 1) indicate that the indexed peaks are related to the  $\text{Fe}_3\text{O}_4$  phase instead of  $\gamma\text{-Fe}_2\text{O}_3$  phase [19, 20].

SEM micrographs and particle size distribution of the as-coprecipitated  $\text{Fe}_3\text{O}_4$  nanoparticles in water and various solvents are given in Fig. 3. The particle size decreases from  $53\pm 17$  to  $33\pm 10$  nm while the particle size distribution becomes slightly narrower by way of using organic solvents instead of water. The particle growth slows down or stops with the adsorbance of organic molecules on the particle surface [11]. Furthermore, the narrower particle size distribution can be attributed to the

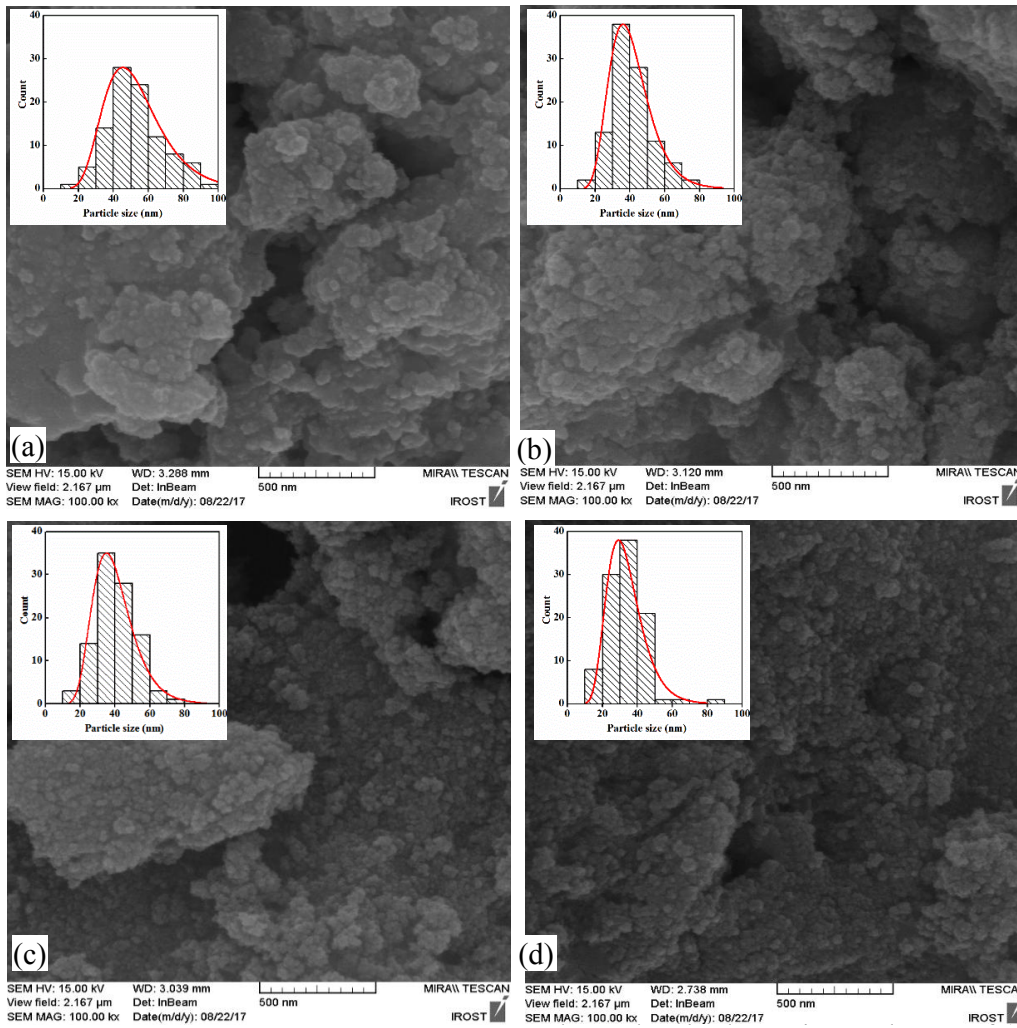


Fig. 3- SEM microstructures of the as-coprecipitated powders in the various solvents of (a)  $\text{H}_2\text{O}$ , (b) EG, (c) DEG and (d) TEG.

separation of nucleation from growth process.

The magnetization curves of the as-coprecipitated  $\text{Fe}_3\text{O}_4$  nanoparticles are shown in Fig. 4. The saturation magnetizations ( $M_s$ ) are also listed in Table 1. The as-coprecipitated  $\text{Fe}_3\text{O}_4$  nanoparticles show ferrimagnetic characteristics which the saturation magnetization increases from 49 to 54 emu/g when using ethylene glycol as solvent and then decreases down to 41 emu/g for triethylene glycol. The magnetic properties of spinel ferrites are strongly dependent on the composition, purity, particle size and shape and cation redistribution [21]. The increase of saturation magnetization by ethylene glycol is due to the increase of crystallinity, while the decrease in  $M_s$  can be attributed to additional decrease in particle size which induced the disordering and spin canting [22]. However, the  $\text{Fe}_3\text{O}_4$  nanoparticles do not have any coercivity, showing their superparamagnetic behavior [23].

#### 4. Conclusions

In this study, single phase magnetite nanoparticles were synthesized by co-precipitation method using organic solvents instead of water. Particle size decreased in the range of 60 to 25 nm and its size distribution became slightly narrower using organic solvent. The highest saturation magnetization of 54 emu/g was obtained by means of ethylene glycol as organic solvent, due to its higher crystallinity. However, the saturation magnetization decreased down to 41 and 45 emu/g for diethylene glycol and triethylene glycol solvents, respectively, due to the spin canting originated from substantial particle refinement.

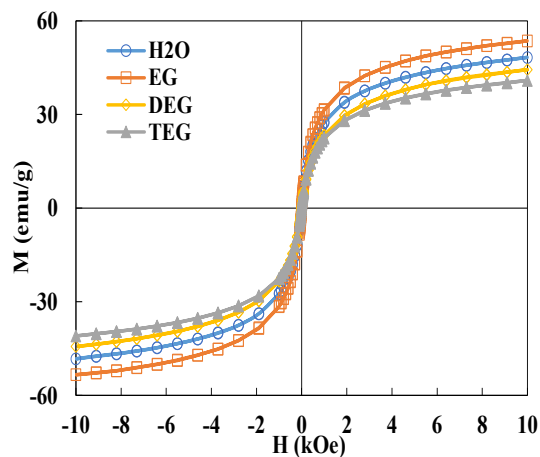


Fig. 4- Magnetization curves of the as-coprecipitated  $\text{Fe}_3\text{O}_4$  powders

#### References

1. Kefeni KK, Msagati TAM, Mamba BB. Ferrite nanoparticles: Synthesis, characterisation and applications in electronic device. *Materials Science and Engineering: B*. 2017;215:37-55.
2. Kobayashi T. Cancer hyperthermia using magnetic nanoparticles. *Biotechnology Journal*. 2011;6(11):1342-7.
3. Liu T-Y, Hu S-H, Liu D-M, Chen S-Y, Chen IW. Biomedical nanoparticle carriers with combined thermal and magnetic responses. *Nano Today*. 2009;4(1):52-65.
4. Guo CX, Huang S, Lu X. A solventless thermolysis route to large-scale production of ultra-small hydrophilic and biocompatible magnetic ferrite nanocrystals and their application for efficient protein enrichment. *Green Chemistry*. 2014;16(5):2571.
5. Gonzales-Weimuller M, Zeisberger M, Krishnan KM. Size-dependant heating rates of iron oxide nanoparticles for magnetic fluid hyperthermia. *Journal of Magnetism and Magnetic Materials*. 2009;321(13):1947-50.
6. Cushing BL, Kolesnichenko VL, O'Connor CJ. Recent Advances in the Liquid-Phase Syntheses of Inorganic Nanoparticles. *Chemical Reviews*. 2004;104(9):3893-946.
7. Alp E, Aydogan N. A comparative study: Synthesis of superparamagnetic iron oxide nanoparticles in air and  $\text{N}_2$  atmosphere. *Colloids and Surfaces A: Physicochemical and Engineering Aspects*. 2016;510:205-12.
8. Shahjuee T, Masoudpanah SM, Mirkazemi SM. Coprecipitation Synthesis of  $\text{CoFe}_2\text{O}_4$  Nanoparticles for Hyperthermia. *Journal of Ultrafine Grained and Nanostructured Materials*. 2017;50(2):105-10.
9. Asuha S, Wan HL, Zhao S, Deligeer W, Wu HY, Song L, et al. Water-soluble, mesoporous  $\text{Fe}_3\text{O}_4$ : Synthesis, characterization, and properties. *Ceramics International*. 2012;38(8):6579-84.
10. Jolivet J-P, Tronc É, Chanéac C. Synthesis of iron oxide-based magnetic nanomaterials and composites. *Comptes Rendus Chimie*. 2002;5(10):659-64.
11. Jolivet JP, Henry M, Livage J. Metal oxide chemistry and synthesis: from solution to solid state. Wiley-Blackwell; 2000.
12. Lee J, Isobe T, Senna M. Preparation of Ultrafine  $\text{Fe}_3\text{O}_4$  Particles by Precipitation in the Presence of PVA at High pH. *Journal of Colloid and Interface Science*. 1996;177(2):490-4.
13. Montazeri-Pour M, Ataie A. Low temperature crystallization of barium ferrite nano-particles via co-precipitation method using diethylene glycol. *International Journal of Modern Physics B*. 2008;22(18n19):3144-52.
14. Montazeri-Pour M, Ataie A, Nikkhal-Moshaie R. Synthesis of Nano-Crystalline Barium Hexaferrite Using a Reactive Co-Precipitated Precursor. *IEEE Transactions on Magnetics*. 2008;44(11):4239-42.
15. Zhang X, Liu J, Yu H, Yang G, Wang J, Yu Z, et al. Enhanced electrochemical performances of  $\text{LiNi}_0.5\text{Mn}_1.5\text{O}_4$  spinel via ethylene glycol-assisted synthesis. *Electrochimica Acta*. 2010;55(7):2414-7.
16. Zhuang L, Zhang W, Zhao Y, Shen H, Lin H, Liang J. Preparation and Characterization of  $\text{Fe}_3\text{O}_4$  Particles with Novel Nanosheets Morphology and Magneto-chromatic Property by a Modified Solvothermal Method. *Scientific Reports*. 2015;5(1).
17. Akbari S, Masoudpanah SM, Mirkazemi SM, Aliyan N. PVA assisted coprecipitation synthesis and characterization of  $\text{MgFe}_2\text{O}_4$  nanoparticles. *Ceramics International*. 2017;43(8):6263-7.
18. Mozaffari S, Li W, Thompson C, Ivanov S, Seifert S, Lee B, et al. Colloidal nanoparticle size control: experimental and kinetic modeling investigation of the ligand-metal binding role in controlling the nucleation and growth kinetics. *Nanoscale*. 2017;9(36):13772-85.
19. Parnianfar H, Masoudpanah SM, Alamolhoda S, Fathi H. Mixture of fuels for solution combustion synthesis of porous  $\text{Fe}_3\text{O}_4$  powders. *Journal of Magnetism and Magnetic Materials*. 2017;432:24-9.
20. Kim W, Suh C-Y, Cho S-W, Roh K-M, Kwon H, Song K, et al. A new method for the identification and quantification of magnetite-maghemite mixture using conventional X-ray diffraction technique. *Talanta*. 2012;94:348-52.

21. Abdel-Mohsen FF, Emira HS. The effect of starting materials and preparation process on the properties of magnesium ferrite pigment. *Pigment & Resin Technology*. 2005;34(6):312-20.
22. Kim J-H, Kim S-M, Kim Y-I. Properties of Magnetic Nanoparticles Prepared by Co-Precipitation. *Journal of Nanoscience and Nanotechnology*. 2014;14(11):8739-44.
23. Reza Barati M, Selomulya C, Suzuki K. Particle size dependence of heating power in MgFe<sub>2</sub>O<sub>4</sub> nanoparticles for hyperthermia therapy application. *Journal of Applied Physics*. 2014;115(17):17B522.